DOI: 10.1002/ejic.200700179

Synthesis, X-ray Structure, Thermal and Magnetic Behavior of $[(bipy)_2Ni_2(\mu\text{-}Cl)_2Cl_2(H_2O)_2]$: The First Neutral Ferromagnetically Coupled Six-Coordinate Dichlorido-Bridged Nickel(II) Dimer

Oluwatayo F. Ikotun,[a] Wayne Ouellette,[a] Francesc Lloret,[b] Miguel Julve,*[b] and Robert P. Doyle*[a]

Keywords: Crystal structures / Nickel complexes / Ferromagnetic coupling / Thermal analysis

$NiCl_2 \cdot 6H_2O$ and 2,2′-bipyridine (bipy) (1:1) were allowed to react under ambient conditions in dimethyl sulfoxide in the presence of acetylacetone (Hacac). The resulting green solution was concentrated in vacuo, and a green solid was isolated by precipitation with cold acetone. X-ray quality crystals of $[(bipy)_2Ni_2(\mu\text{-}Cl)_2(Cl)_2(H_2O)_2]$ (**1**) were grown by subsequent vapor/liquid diffusion of acetonitrile into a methanolic solution for one week. The structure of **1** consists of a dimeric nickel system with each metal atom in an octahedral geometry. Both equatorial bridging and axial chlorine atoms are present in this neutral species. The nickel–nickel distance (3.441 Å) is the shortest reported to date for this class of complexes and the bridging chlorido angles at 91.5° are the most acute. Variable-temperature magnetic susceptibility measurements reveal the complex to have the strongest ferromagnetic interaction reported to date (J = +16.8 cm^{-1}, the Hamiltonian being defined as $H = -JS_A \cdot S_B$) for this family of complexes.

Introduction

Multimetallic nickel(II) species occupy an important position in modern inorganic and materials chemistry. They are ubiquitous in nature as active sites in a variety of metallo-enzymes and this recognition has fuelled the development of numerous low molecular weight model compounds.[1] In addition, they have been investigated from the viewpoint of magnetochemistry, in particular in the prediction of superexchange coupling between paramagnetic centers.[2] In this field the seminal work on structure/function correlation remains that by Hatfield and Hodgson who found a linear correlation between the strength and sign of the magnetic interaction and the bridging angle, θ, for eight, essentially planar, di-μ-hydroxidodicopper(II) complexes.[3] This was further expanded by Ruiz et al. to include the effects of the out-of-plane dispersion of the hydroxido hydrogen atom resulting in a highly successful predictor of magnetic behaviour in this class of compounds.[1] Such a correlation, with clear predictors, has yet to be established for five- and six-coordinate di-μ-chloridodinickel(II) complexes. Reedijk et al. have produced a comprehensive review of such structures and their magnetic behaviour[4] but attempts to produce a structure/function correlation have been hampered by the dearth of such complexes in the literature, especially complexes that are unique or extreme in geometry, bridging angle, nickel–nickel distance, charge, etc. Goodenough, Kanamori, and Anderson predicted that with an octahedral geometry and an M–X–M bridging angle close to 90°, a ferromagnetic coupling between two d^8 metal ions would be observed.[5] Theoretical studies by Barraclough and Brookes[6] and work by Gatteschi et al.[7] have also concluded that close proximity of the bridging Ni–Cl–Ni angle to 90° was a strong predictor of a ferromagnetic interaction. They also noted, however, that distortions about the octahedral metal ion would increase antiferromagnetic character by mixing d orbitals, and this sensitivity would make predicting the coupling strength and sign difficult for such systems. A search of the literature revealed only six ferromagnetic di-μ-chloridodinickel(II) complexes that have been both magnetically and structurally characterized with the most acute bridging angle noted to date between the Ni–Cl–Ni atoms being 93.03°.[8] Two of the six complexes with intramolecular ferromagnetic coupling are five-coordinate, distorted trigonal-bipyramidal with the remaining four having octahedral geometry. Both the five-coordinate structures show a high degree of distortion from perfect square-pyramidal geometry (as measured by τ and compared to analogous complexes displaying antiferromagnetic behaviour).[9] Reedijk et al. have noted this may be the

[a] Department of Chemistry, Syracuse University, Syracuse, NY 13244-4100, USA
E-mail: rpdoyle@syr.edu
[b] Department of Química Inorgànica/Instituto de Ciencia Molecular, Universitat de València, Polígono La Coma s/n, 46980 Paterna (València), Spain
E-mail: miguel.julve@uv.es

Supporting information for this article is available on the WWW under http://www.eurjic.org or from the author.

source of the strengthening of the ferromagnetic coupling in five-coordinate structures (again distortion playing an important role).[4] All the octahedral ferromagnetic complexes are charged and no such neutral structures have been characterized. Such a structure, devoid of counterion-induced distortions, that exhibits close proximity to 90°, would be an intriguing result, because current predictors would charge that this structure be strongly ferromagnetic (certainly stronger than any such value of ferromagnetic coupling reported to date). In this paper we present a new octahedral dichlorido-bridged nickel(II) dimer, $[(bipy)_2Ni_2(\mu\text{-}Cl)_2(Cl)_2(H_2O)_2]$ (**1**), with the most acute Ni–Cl–Ni bridging angle (91.5°) and the shortest intramolecular Ni···Ni distance (3.44 Å) observed to date. These extremes and the fact that it is the first neutral octahedral complex in this family, makes this structure somewhat of a "missing link" for such di-μ-chloridodinickel(II) complexes.

Results and Discussion

Synthesis of $[(bipy)_2Ni_2(\mu\text{-}Cl)_2(Cl)_2(H_2O)_2]$ (1)

The compound was synthesized from nickel(II) chloride hexahydrate and 2,2′-bipyridine (bipy) in a stoichiometric ratio of 1:1 in the presence of acetylacetone (Hacac). Interestingly, attempts to obtain **1** without the presence of Hacac failed, instead producing a blue solid for which a crystal structure is currently being sought. Our desire to follow this reaction stems from our observation that in reactions involving attempts to incorporate pyrophosphate ($P_2O_7^{4-}$) into $(bipy)Ni^{II}$ systems, dichlorido "impurities" were observed when the chloride salt was used. We wanted to know if we could prepare this complex directly and subsequently conduct full structural and functional characterization.

Characterization of 1

The IR spectrum of **1** is consistent with the presence of coordinated 2,2′-bipyridine.[17] Electrospray mass spectrometry revealed the presence of Cl isotopes and is consistent with the presence of **1** as the monocationic acetonitrile solvate $\{[(bipy)_2Ni_2(\mu\text{-}Cl)_2Cl(H_2O)_2]\cdot MeCN\}^+$. Elemental analysis (C, H, N) is also consistent with the formula of **1**. The extinction coefficient (H_2O) was calculated to be 3.4 $M^{-1}\,cm^{-1}$ for both Ni^{II} atoms, a value, which is indicative of the presence of an octahedral structure in solution.

Description of the Crystal Structure of 1

The structure of **1** consists of neutral $(bipy)NiCl_2(H_2O)$ units, which are related by the crystallographic center of symmetry, as shown in Figure 1.

The crystallographically independent unit consists of an Ni^{II} ion, octahedrally surrounded by two N atoms from the bipyridine ligand [Ni(1)–N(1) = 2.048 Å and Ni(1)–N(2) = 2.053 Å], one coordinated water molecule [Ni(1)–O(90) = 2.14 Å], and three chlorine atoms (one axial chlorido group [Ni(1)–Cl(2)] and two bridging equatorial chlorido groups [Ni(1)–Cl(1) and Ni(1)–Cl(1a)]). The *trans*-axial bridging angles [Cl(2)–Ni(1)–O(90)] show only a slight deviation from linearity at 176°. The Ni–Cl–Ni bridging unit is practically planar and the dimer is located on an inversion center.

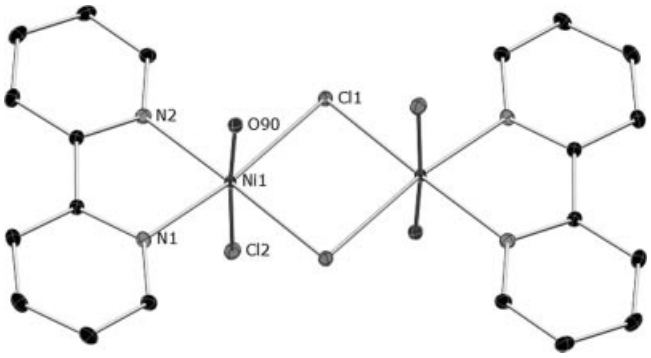

Figure 1. ORTEP plot of **1** with the atom labeling scheme; hydrogen atoms have been removed for clarity; the unlabeled atoms are generated by an inversion center. Thermal ellipsoids are plotted at 50% probability level.

Table 1. Comparison between structural and magnetic data of di-μ-chloridodinickel(II) complexes.[a]

Compound	Ni–Cl–Ni [°]	Ni···Ni [Å]	Ni–Cl_{bridge} [Å]	Ni–Cl_{bridge} [Å]	Space group	J [cm^{-1}]	Ref.
Square-pyramidal or trigonal-bipyramidal							
$[Ni(biq)Cl_2]_2$	96.68(2)	3.563(1)	2.372(1)	2.400(1)	$\bar{P}$	–7.74	[10]
$[Ni(dmp)Cl_2]_2$	97.4(1)	3.600(1)	2.378(1)	2.414(1)	$\bar{P}$	–5.1	[10]
$[Ni(qnqn)Cl_2]_2$	98.23(5)	3.652(1)	2.408(2)	2.422(2)	$\bar{P}$	–4.4	[11,12]
$[NiCl_2(pqo)]_2$	95.84(8)	–	2.337(2)	2.387(2)	$P2_1/n$	–0.632	[13]
$[NiCl_2\{CH_2(dmpz)_2\}]_2$	97.36(4)	3.587(2)	2.318(1)	2.456(1)	$\bar{P}$	+2.58	[2a]
$[NiCl_2(tbz)_2]_2\cdot 2C_2H_6O$	97.23(6)	3.5891(12)	2.3556(17)	2.4275(16)	$P2_1/c$	+2.5	[4]
Octahedral							
$[Ni(en)_2Cl]_2Cl_2$	94.1	3.67	2.461(3)	2.551(3)	$P2_1/n$	+9	[14]
$[Ni(en)_2Cl]_2(ClO_4)_2$	95.4	–	2.461(3)	2.512(3)	$P2_1/n$	+8.9	[14]
$[Ni(EG)_2Cl]_2Cl_2$	93.03(5)	3.458(1)	2.383(1)	2.383(1)	$C2/m$	+5.5	[8]
$(PDA)_2[NiCl_4(H_2O)]_2$	95.05(5)	3.606(2)	2.430(2)	2.459(1)	$C2/c$	+8.2	[15,16]

[a] Abbreviations: biq = 2,2′-biquinolyl, dmp = 2,9-dimethyl-1,10-phenanthroline, qnqn = *trans*-2-(2′-quinolyl)methylene-3-quinuclidinone, pqo = 2-(pyrid-2-yl)quinoxaline, dmpz = 3,5-dimethylpyrazolyl, tbz = 2-benzimidazolyl, EG = ethyleneglycol, PDA = 1,3-propylenediammonium. Table adapted from ref.[4]

The separation between the Ni ions is 3.441 Å and the Ni–Cl–Ni angle is 91.5°, both are extreme values for this family of complexes (see Table 1). The interior Cl(1)–Ni(1)–Cl(1a) angle is 88.4° with Cl(1)···Cl(1a) intramolecular distance being 3.348 Å. Further selected bond lengths and angles are given in Table 2.

Table 2. Selected bond lengths [Å] and angles [°] for **1**.

Ni(1)–N(1)	2.0483(12)	N(1)–Ni(1)–N(2)	79.60(5)
Ni(1)–N(2)	2.0535(11)	N(1)–Ni(1)–Cl(1)	95.90(3)
Ni(1)–O(90)	2.1394(10)	O(90)–Ni(1)–Cl(1)	84.60(3)
Ni(1)–Cl(1)	2.3957(4)	O(90)–Ni(1)–Cl(2)	176.04(3)
Ni(1)–Cl(1a)	2.4048(4)	Cl(1)–Ni(1)–Cl(2)	91.532(13)
Ni(1)–Cl(2)	2.4383(4)	Ni(1)–Cl(1)–Ni(1a)	91.564(13)
Torsion angles:			
N(2)–N(1)–Cl(2)–Cl(2)	1.62		
N(2)–N(1)–Ni(1)–Cl(2)	54.75		

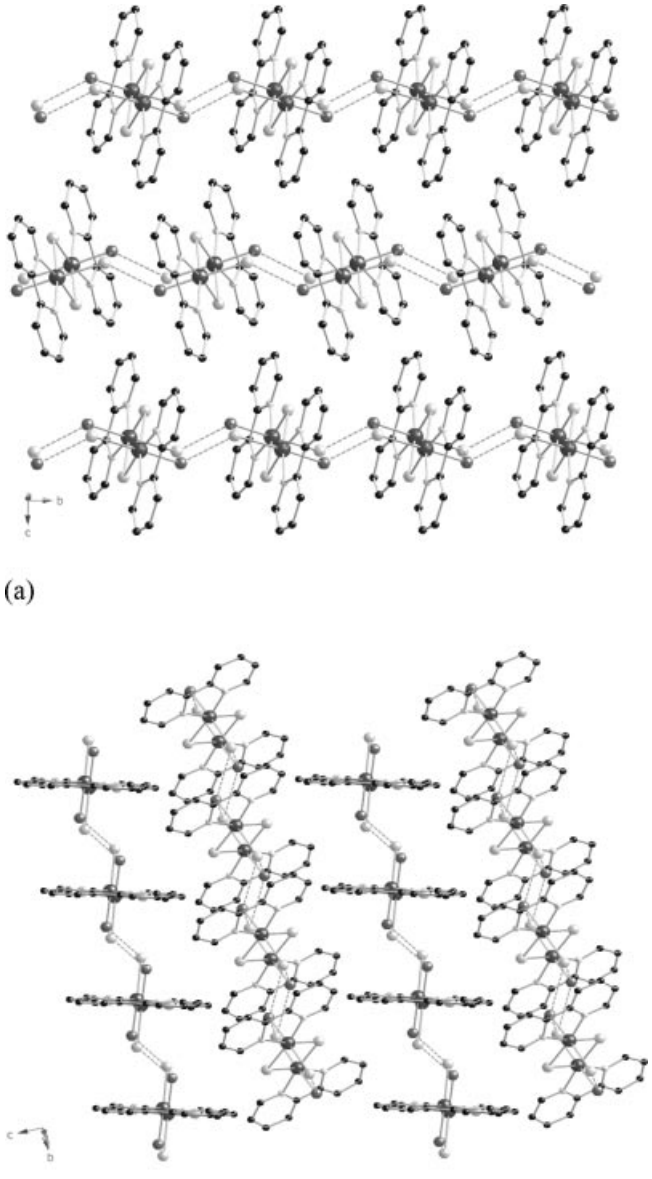

Figure 2. (a) Packing diagram of **1** looking along the crystallographic *b* axis; note the alternating arrangement of intermolecular hydrogen bonds. (b) Looking along the crystallographic *c* axis. Hydrogen atoms have been omitted for clarity.

Average carbon–carbon and carbon–nitrogen bond lengths of the coordinated 2,2′- bipyridine are close to those reported for the free molecule.[18] The significant deviation of the N(1)–Ni–N(2) angle [79.60(5)°] from the ideal value (90°) is due to steric requirements of a bipyridine ring ligand. Interestingly, complex **1** packs to produce 1-dimensional alternating ABAB layers of asymmetric units along the crystallographic *b* axis. Within each individual layer the asymmetric units are connected through intermolecular hydrogen bonds between the coordinated water and chlorine atoms of adjacent dimers. The intermolecular O_w···Cl distance of 3.195 Å is typical of an O–H···Cl interaction (range of 2.95–3.30 Å). The torsional angle between intralayer bipyridine rings is ca. 180°, indicating a near perfect parallel alignment within each layer. Closest distance between such bipyridine rings, however, is ca. 6.4 Å indicating that intralayer π–π stacking is not present in **1**. Interlayer distances, however, approach 3.7 Å with the phenanthroline rings interleaving such that the edge of one ring interacts with the face of another, both consistent with *phenyl embraces*.[19] Certainly, the complex packs to produce clear hydrophobic and hydrophilic regions, and their combination helps to explain the "twist" between layers in **1** as shown in Figure 2 (b).

Magnetic Behavior of 1

Variable-temperature magnetic susceptibility studies were carried out on a powdered sample of the crystalline complex **1** over the temperature range 1.9–300 K. The magnetic behavior of **1** is shown in Figure 3 in the form of a $\chi_M T$ vs. T plot [χ_M being the magnetic susceptibility per two nickel(II) ions]. The value of $\chi_M T$ at room temperature, ca. 2.30 $cm^3 mol^{-1}$ K, is as expected for two single-ion triplet states magnetically isolated ($\chi_M T$ = 2.31 $cm^3 mol^{-1}$ K with g = 2.15). This value continuously increases upon cooling to reach a maximum of 4.10 $cm^3 mol^{-1}$ K at 5.0 K and then further decreases to 3.68 $cm^3 mol^{-1}$ K at 1.9 K. The shape of this curve is typical of a significant ferromagnetic coupling in **1**, the decrease of $\chi_M T$ at low temperatures being due to zero-field splitting effects and/or intermolecular interactions. In addition, the fact that $\chi_M T$ at low temperatures reaches values larger than 3.50 $cm^3 mol^{-1}$ K (the calculated value for a magnetically isolated quintet spin state with g = 2.09) supports the occurrence of interdimer ferromagnetic interactions in **1**. Most likely, the hydrogen bonds, which link the dimers to afford a chain of dinuclear nickel(II) units along the crystallographic *a* axis [see Figure 2 (a)] provide the exchange pathway for this additional ferromagnetic interaction.

Keeping in mind the dinuclear structure of **1** and the fact that the ground state for a nickel(II) ion in an octahedral environment is orbitally nondegenerate, it is possible to represent the intradimer magnetic interaction J with the iso-

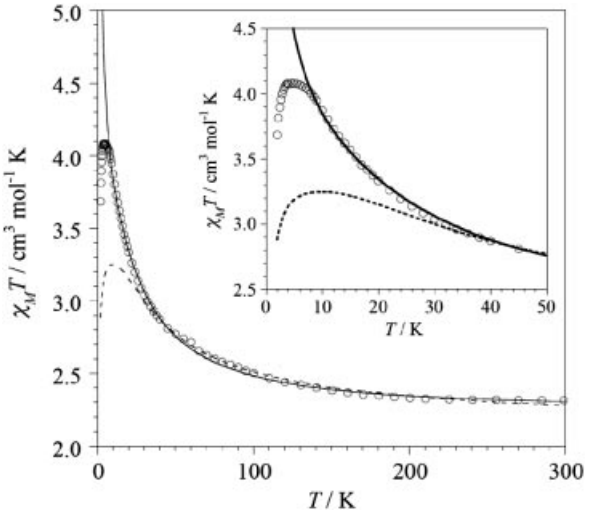

Figure 3. $\chi_M T$ vs. T plot for **1**: experimental data (circles); best-fit curve for a nickel(II) dimer with J, g and D as variable parameters (dashed line); best-fit curve for a uniform chain of nickel(II) dimers (solid line) (see text). The inset shows the low-temperature region in detail.

tropic spin Hamiltonian $H = -JS_A \cdot S_B$. This approach works well for the cases where a relatively strong antiferromagnetic coupling is involved. However, when a weak antiferromagnetic interaction occurs or when the coupling is ferromagnetic (as in **1**), the effect of D [zero-field splitting of the octahedral nickel(II) ion] has to be taken into account to describe the magnetic behaviour at low temperatures.[20]

We have then analyzed the magnetic susceptibility data of **1** in the high-temperature range by the corresponding expression derived through the Hamiltonian of Equation (1).[20]

$$H = -JS_A \cdot S_B + D(S_{zA}^2 + S_{zB}^2) \quad (1)$$

The best-fit values are: $J = +16.8$ cm^{-1}, $g = 2.09$ and $D = 3.5$ cm^{-1}. The calculated plot corresponds to the dashed line in Figure 3. The theoretical curve reproduces the experimental data from room temperature to $T = 40$ K. At $T < 40$ K, there is a clear mismatch between the experimental data and the theoretical plot, the former being above the calculated curve. This is in agreement with the additional ferromagnetic interaction between the nickel(II) dimers through the hydrogen bonds mentioned above. As the spin of the ferromagnetically coupled nickel(II) dimer at $T \leq 40$ K is large enough ($S \approx 2.0$) to be considered as a classic one, the magnetic data of **1** in the low-temperature range could be modelled through a uniform chain of hydrogen-bonded nickel(II) dimers (denoted P) with an interdimer ferromagnetic coupling j_{eff}, the Hamiltonian being defined by Equation (2).

$$H_{eff} = -j_{eff} \Sigma_i (S_{P,i} \cdot S_{P,i+1}) \quad (2)$$

The value of the spin of each P unit (S_P) is given by Equation (3), where χ_P is the magnetic susceptibility for the nickel(II) dimer derived through Equation (1)[19] and g_P is the g factor for the ground spin sate of the dimer which is the local g factor of the nickel(II) ion.

$$S_P(S_P + 1) = 8\chi_P T/g_P \quad (3)$$

In such an approach of a classical spin Heisenberg chain model,[21] the expression for the magnetic susceptibility per P unit is given by Equations (4), (5) and (6).

$$\chi_P = [N\beta^2 g_P^2 S_P(S_P + 1)/3kT]\{[1 + u(K)]/[1 - u(K)]\} \quad (4)$$

$$u(K) = \coth(K - 1)/K \quad (5)$$

$$K = j_{eff} S_P(S_P + 1)/kT \quad (6)$$

This approach allowed us to fit the magnetic data of **1** from room temperature to $T = 8.0$ K (solid line in the inset of Figure 3), the values of the best-fit parameters being $J_P = +16.8$ cm^{-1}, $g_P = 2.09$, $D = 3.5$ cm^{-1} and $j_{eff} = +0.37$ cm^{-1}. The previous values of J, g and D remain unchanged in the new fit and the weak ferromagnetic coupling (j_{eff}) between the nickel(II) dimers through the hydrogen bonds is evaluated. The very small j_{eff}/J_P ratio (ca. 0.02) supports the validity of the perturbational model used here.

Such an approach was successfully used by some of us in other magnetic systems.[22–26] The mismatch between the calculated curve and the experimental data at $T < 8.0$ K for **1** in Figure 3 is most likely due to weak interchain antiferromagnetic interactions, which certainly would cause a decrease of the magnetic moment in the very-low-temperature region. We should also note that although the simulation of the magnetisation (M) vs. the applied magnetic field (H) plots for a discrete molecule with J (magnetic coupling) and D (zero-field splitting) as variable parameters is possible for a discrete molecule, it cannot be used for a chain (as is the case here). Consequently, M vs. H plots for **1** were discarded. Finally, the decrease of the $\chi_M T$ product being due to saturation phenomena (Zeeman level depopulation effects) was also discarded because the plots for three H values less than 500 G (that is 250, 100 and 50 G) provided the same susceptibility curve.

Conclusion

We report the first neutral octahedral di-μ-chloridodinickel(II) complex with the most acute Ni–Cl–Ni bridging angle to date. The complex exhibits the strongest intramolecular ferromagnetic interaction for this family, as expected given the acute bridging angle and quasi-planarity of the bridging unit, and is an important addition to this family of complexes.

Experimental Section

General: Solvents and chemicals were of laboratory grade and were used as received except dimethyl sulfoxide, which was dried with molecular sieves (4 Å) under dry dinitrogen. Electrospray mass spectrometry was performed with a Shimadzu LCMS-2010 A system at a cone voltage of 5 kV. Infrared spectra were recorded with a

Nicolet Magna-IR 850 Series II spectrophotometer as KBr pellets. Thermal analysis was performed with a TA instruments TGA Q500 using 2–6 mg samples placed on platinum pans and ran under nitrogen (40 mL/min). The temperature was ramped from ca. 25 to 500 °C at a rate of 10 °C/min. Analysis was performed using the TA instruments Universal Analysis 2000 software program. Elemental analysis (C, H, N) was performed by Quantitative Technologies Inc., Whitehouse, NJ. Water was distilled and deionized to 18.6 MΩ using a Barnstead Diamond RO Reverse Osmosis machine coupled to a Barnstead Nano Diamond ultrapurification machine. Variable-temperature magnetic susceptibility measurements were performed with a Quantum design SQUID susceptometer in the temperature range 1.9–300 K with an applied magnetic field of H = 1000 G ($T \geq 100$ K) and 50 G ($T < 100$ K). Crystalline samples were obtained directly from the reaction mixture, air-dried and powdered in a mortar. Diamagnetic corrections for the constituent atoms were estimated using Pascal's constants and corrections for the sample holder and the temperature-independent paramagnetism were also performed. Electronic absorption spectra were obtained with a Varian Cary 50 Bio spectrophotometer in 1-mL Quartz cuvettes between 200 and 800 nm at ambient temperature.

Synthesis and Characterization of $[(bipy)_2Ni_2(\mu\text{-}Cl)_2(Cl)_2(H_2O)_2]$ (1): $NiCl_2$ (0.48 g, 2.0 mmol) was suspended in dimethyl sulfoxide (DMSO) (10 mL). To this was added acetylacetone (10 mL, 99.3%) and then 2,2′-bipyridine (0.31 g; 2.0 mmol) was added as a 10-mL solution in DMSO. The volume of the solution was reduced in vacuo to approximately 5 mL, and a green solid was precipitated with chilled acetone. The precipitate was subsequently dissolved in a minimum amount of methanol and filtered (0.45 μm Fisher). Crystallization was conducted by an acetonitrile/methanol diffusion performed under ambient conditions. Green block-shaped crystals grew over ca. 8 d. Yield 0.941 g (41% based on Ni^{II}). $C_{20}H_{20}Cl_4N_4Ni_2O_2$ (607.6): calcd. C 39.50, H 3.32, N 9.22; found C 39.24, H 3.18, N 9.06. λ_{max} (H_2O) = 612 nm (3.4 $M^{-1}cm^{-1}$). FT-IR (KBr): $\tilde{\nu}$ = 1598 (s), 1475 (s), 1445 (s), 1313 (m), 1115 (w), 1057 (w), 1027 (w), 775 (s), 736 (m), 654 (w) cm^{-1}. ES-MS (90% MeOH/10% H_2O): m/z = 612 $\{[(bipy)_2Ni_2(\mu\text{-}Cl)_2(Cl)(H_2O)_2]\cdot MeCN\}^+$.

Crystal-Structure Determination and Refinement for 1: Structural measurements were performed with a Bruker-AXS SMART-CCD diffractometer at low temperature (90 K) using graphite-monochromated Mo-K_α radiation (λ = 0.71073 Å). Absorption correction was applied using SADABS and SHELXTL and the structure was solved by direct methods and refined using the SHELXTL program package.[27] Key crystallographic data are given in Table 3. CCDC-631084 contains the supplementary crystallographic data for this paper. These data can be obtained free of charge from The Cambridge Crystallographic Data Centre via www.ccdc.cam.ac.uk/data_request/cif.

Table 3. Crystal data for $[(bipy)_2Ni_2(\mu\text{-}Cl)_2(Cl)_2(H_2O)_2]$ (**1**).

Empirical formula	$C_{20}H_{20}Cl_4N_4Ni_2O_2$
Formula mass	607.602
Crystal system	monoclinic
Space group	$P2_1/n$
μ (Mo-K_α) [mm^{-1}]	2.173
a [Å]	11.0985(9)
b [Å]	6.7873(6)
c [Å]	14.9609(12)
β [°]	91.900(2)
V [Å^3]	1126.37(16)
Z	2
$D_{calcd.}$ [gcm^{-3}]	1.792
F[000]	616
T [K]	175
θ_{max}	28.07
R, wR_2 [$I > 2\sigma(I)$]	0.0202, 0.0510
R, wR_2 (all data)	0.0211, 0.0516
Total data, total unique data	11216, 2733
Observed data [$I > 2\sigma(I)$]	2733
No. of final reflections, parameters	2733, 185
Final R_1, wR_2	0.0202, 0.0510

Supporting Information (see footnote on the first page of this article): Thermal analysis of **1**.

Acknowledgments

Thanks are due to Promega Corporation (Madison, WI, USA), the iLEARN Program, Syracuse University and the Ministerio Español de Ciencia y Tecnología (Project BQU2004-03633) for funding.

[1] a) E. Ruiz, P. Alemany, S. Alvarez, J. Cano, *Inorg. Chem.* **1997**, *36*, 3683; b) E. Ruiz, P. Alemany, S. Alvarez, J. Cano, *J. Am. Chem. Soc.* **1997**, *119*, 1297.
[2] a) J. C. Jansen, H. van Koningsveld, J. A. C. van Ooijen, J. Reedijk, *Inorg. Chem.* **1980**, *19*, 170; b) J. Reedijk, J. Verbiest, *Transition Met. Chem.* **1978**, *3*, 51; c) R. P. Doyle, P. E. Kruger, M. Nieuwenhuyzen, B. Moubaraki, K. S. Murray, *Dalton Trans.* **2003**, 4230; d) P. E. Kruger, G. D. Fallon, B. Moubaraki, K. J. Berry, K. S. Murray, *Inorg. Chem.* **1995**, *34*, 4808; e) R. P. Doyle, P. E. Kruger, M. Julve, F. Lloret, M. Nieuwenhuyzen, *Dalton Trans.* **2006**, 2081; f) R. P. Doyle, M. Nieuwenhuyzen, P. E. Kruger, *Dalton Trans.* **2005**, 3745; g) R. P. Doyle, P. E. Kruger, M. Julve, F. Lloret, M. Nieuwenhuyzen, *CrystEngComm* **2002**, *4*, 13; h) R. P. Doyle, P. E. Kruger, M. Julve, F. Lloret, M. Nieuwenhuyzen, *Inorg. Chem.* **2001**, *40*, 1726.
[3] V. H. Crawford, H. W. Richardson, J. R. Wasson, D. J. Hodgson, W. E. Hatfield, *Inorg. Chem.* **1976**, *15*, 2107.
[4] G. A. Van Albada, J. J. A. Kolnaar, W. J. J. Smeets, A. L. Spek, J. Reedijk, *Eur. J. Inorg. Chem.* **1998**, *9*, 1337.
[5] a) J. B. Goodenough, *Phys. Rev.* **1955**, *100*, 564; b) J. Kanamori, *J. Phys. Chem. Solids* **1959**, *10*, 87; c) P. W. Anderson, *Phys. Rev.* **1959**, *115*, 2.
[6] C. G. Barraclough, R. W. Brookes, *J. Chem. Soc., Faraday Trans.* **1974**, *2*, 1364.
[7] A. Bencini, D. Gatteschi, *Inorg. Chim. Acta* **1978**, *31*, 11.
[8] B. M. Antti, *Acta Chem. Scand. Ser. A* **1975**, *29*, 76.
[9] A. W. Addison, T. N. Rao, J. Reedijk, J. Van Rijn, G. C. Verschoor, *J. Chem. Soc., Dalton Trans.* **1984**, 1349.
[10] R. J. Butcher, E. Sinn, *Inorg. Chem.* **1977**, *16*, 2334.
[11] E. J. Laskowski, T. R. Felthouse, D. N. Hendrickson, G. J. Long, *Inorg. Chem.* **1976**, *15*, 2908.
[12] G. J. Long, E. O. Schlemper, *Inorg. Chem.* **1974**, *13*, 279.
[13] C. Shao, W. Sun, Y. Chen, R. Wang, C. Xi, *Inorg. Chem. Commun.* **2002**, *5*, 667.
[14] G. A. Bottomley, L. G. Glossop, C. L. Raston, A. H. White, A. C. Willis, *Aust. J. Chem.* **1978**, *31*, 285.
[15] C. P. Landee, R. D. Willett, *Inorg. Chem.* **1981**, *20*, 2521.
[16] D. Knetsch, W. L. Groeneveld, *Inorg. Nucl. Chem. Lett.* **1976**, *12*, 27.
[17] K. Nakamoto, *Infrared Spectra of Inorganic and Coordination Compounds*, John Wiley & Sons, Inc., New York, **1963**.
[18] L. L. Merrit, E. D. Schroeder, *Acta Crystallogr.* **1956**, *9*, 801.
[19] I. Dance, M. Scudder, *J. Chem. Soc., Chem. Commun.* **1995**, 1039.
[20] G. De Munno, M. Julve, F. Lloret, A. Derory, *J. Chem. Soc., Dalton Trans.* **1993**, 1179.
[21] M. E. Fisher, *Am. J. Phys.* **1964**, *32*, 343.
[22] F. Lloret, M. Julve, R. Ruiz, Y. Journaux, K. Nakatani, O. Kahn, J. Sletten, *Inorg. Chem.* **1993**, *32*, 27.

[23] F. Lloret, R. Ruiz, M. Julve, J. Faus, Y. Journaux, I. Castro, M. Verdaguer, *Chem. Mater.* **1992**, *4*, 1150.
[24] F. Lloret, R. Ruiz, B. Cervera, I. Castro, M. Julve, J. Faus, J. A. Real, F. Sapiña, Y. Journaux, J. C. Colin, M. Verdaguer, *J. Chem. Soc., Chem. Commun.* **1994**, 2615.
[25] L. K. Thompson, S. S. Tandon, F. Lloret, M. Julve, J. Cano, *Inorg. Chem.* **1997**, *36*, 3301.
[26] Y. Rodríguez-Martin, C. Ruiz-Pérez, J. Sanchiz, F. Lloret, M. Julve, *Inorg. Chim. Acta* **2001**, *318*, 159.
[27] *SHELXTL PC*, version 6.1, Bruker-AXS, Inc., Madison, WI, USA, **2002**.

Received: February 6, 2007
Published Online: March 27, 2007

